Inorganic Chemistry

FORUM ARTICLE

pubs.acs.org/IC

Molecular Hume−Rothery Compounds $[M(ZnR)_n]$ and $[M(ZnR)_a(GaR)_b]$ ($a + 2b = n \geq 8$): Relations of Coordination Polyhedra and Electronic Structure

Mariusz Molon,[†] Christian Gemel,[†] Moritz von Hopffgarten,[‡] Gernot Frenking,*[,‡] and Roland A. Fischer*[,†]

[†]Anorganische Chemie II, Organometallics & Materials, Ruhr-Universität Bochum, D-44780 Bochum, Germany

[‡]Fachbereich Chemie, Philipps-Universität Marburg, Hans-Meerwein-Strasse, D-35043 Marburg, Germany

Supporting Information

ABSTRACT: The icosahedral complex $[Mo(ZnMe)_9(Zn\text{-}Cp^*)_3]$ is discussed as the prototype for a whole family of high-coordinate, metal-rich compounds $[M(ZnR)_n]$ and $[M(ZnR)_a(GaR)_b]$ ($a + 2b = n \geq 8$; for the same metal M). In contrast to other highly coordinate complexes of classic, monodentate (nonchelating) nonmetal atom ligator ligands, for the (weakly) bonding metal atom ligators ZnR and GaR, attractive ligand−ligand interactions play an important role. The structures of the compounds were evaluated by the method of continuous-shape measures, and the bonding situation of models (R = H) was analyzed on the density functional level of theory. The structures and coordination polyhedra of $[M(M'R)_n]$ (M′ = Zn, Ga) turned out to be *independent* of the central metal or the nature of the metals M′ in the ligand shell, and the resulting molecular orbital schemes vary only slightly as a result of the different symmetries, however resulting in the same coordination polyhedra (structures) for all complexes. This result may be viewed as a molecular representation for the situation in extended solid-state intermetallic phases of the Hume−Rothery type.

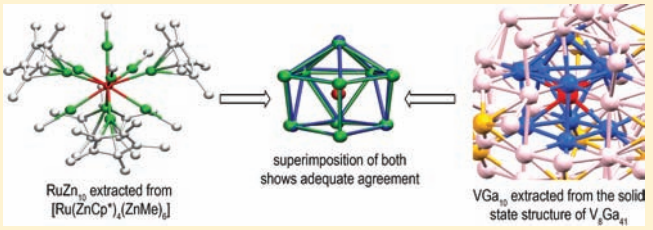

1. INTRODUCTION

Coordination polyhedra of transition-metal complexes are usually derived from the electron count of their central metals. A change in the coordination polyhedra of the metal leads to a different d-orbital splitting and thus to an electronic stabilization or destabilization of the whole complex. Simple models such as the ligand-field theory allow a quick assessment of possible structures and assignment of the most stable one.[1−4] However, this is especially true for low-coordinate complexes (CN ≤ 6), where ligand−ligand interactions can be neglected and changes in symmetry have a large effect on the orbital splitting. For highly coordinated complexes, it is generally believed that the d-electron count of the central metal has only marginal effects on the structure, but instead ligand−ligand repulsion and packing effects (or cation−anion interactions, respectively) determine the coordination polyhedron around the central atom.[3,5−7]

Quite recently, a new family of highly coordinated complexes, the metal-rich compounds $[M(ZnR)_n]$, $[M(CdR)_n]$, and $[M(ZnR)_a(CdR)_b]$ ($a + b = n$), have been discovered ($n \geq 8$; M = Mo, Ru, Rh, Ni, Pd, Pt; R = CH_3, C_2H_5, Cp*).[8−11] The formation of these Zn (Cd)-rich compounds is accomplished by selective Ga/Zn and Cp*/Me exchange reactions starting from homoleptic complexes $[M(GaCp^*)_n]$ and ZnR_2 (CdR_2). All of these reactions lead to the substitution of one GaCp* ligand by two ZnR ligands, formally best described as a redox reaction in which Ga^{I} is oxidized to Ga^{III}, while Zn is reduced from II+ to I+. The reactions, presumably proceeding via radical reaction mechanisms, lead to the formation of GaR_3 as side products, which can be identified by NMR spectroscopy in many cases.

These compounds may serve as suitable models linking mixed-metal complexes and clusters, on the one hand, and the respective solid-state intermetallic phases, i.e., Hume−Rothery-type alloys, on the other hand.[12] Although a series of homoleptic compounds $[M(ZnR)_n]$ have been prepared, only two heteroleptic examples with the traditional organometallic spectator ligands Cp* and CO are known, so far: Treatment of $[(CO)_4Mo(GaCp^*)_2]$ or $[Cp^*Rh(GaCp^*)_2(GaCl_2Cp^*)]$ with $ZnMe_2$ leads to complex molecules with four or six transition metals connected via M−Zn−M bridging units resulting in molecular compositions of $[\{(CO)_4Mo\}_4(Zn)_6(\mu_2\text{-}ZnCp^*)_4]$[12] and $[Cp^*_2Rh][(Cp^*Rh)_6Zn_6(ZnCl)_{12}(\mu_6\text{-}Cl)]$,[13] respectively. Most interestingly, it has been shown that the structure of the Mo_4Zn_6 metal core of $[\{(CO)_4Mo\}_4(Zn)_6(\mu_2\text{-}ZnCp^*)_4]$ represents a molecular cutout of the structurally characterized Zn-rich intermetallic Hume−Rothery phase $MoZn_{20.44}$.

Analysis at the density functional level of theory (DFT) suggested the bonding situation in these compounds to lie between complexes and clusters; i.e., the radial M−Zn and tangential Zn−Zn interactions both contribute to the stability of the compounds (however, these cannot be described as interstitial cage molecules, $M@Zn_n$). The isolobal relationship H/ZnR and

Received: April 19, 2011
Published: July 12, 2011

dx.doi.org/10.1021/ic200800e | *Inorg. Chem.* 2011, 50, 12296–12302

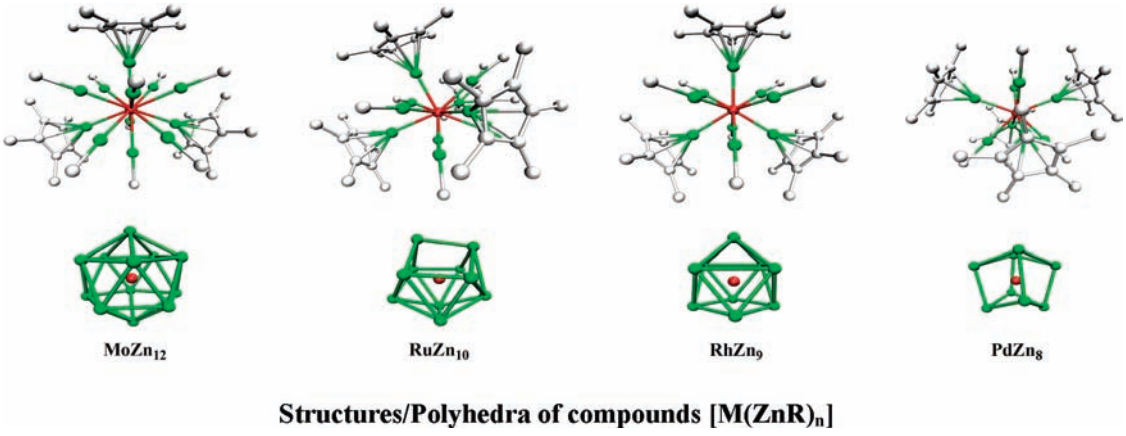

Figure 1. Perspective plot of the molecular structures $[Mo(ZnCp^*)_3(ZnMe)_9]$, $[Ru(ZnCp^*)_4(ZnMe)_6]$, $[Rh(ZnCp^*)_3(ZnMe)_6]$, and $[Pd(ZnCp^*)_4(ZnMe)_4]$ in the solid state with the corresponding metal-core polyhedra **$MoZn_{12}$**, **$RuZn_{10}$**, **$RhZn_9$**, and **$PdZn_8$** at the bottom. Color code: transition metals, red; Zn, green; C, gray.

the corresponding chemical analogy H/Au suggest a certain congruence between the new $[M(ZnR)_n]$ systems and the corresponding homoleptic hydrides MH_n and the central metal M "doped" gold clusters MAu_n, respectively. Indeed, the molecular compound $[Mo(ZnCp^*)_9(ZnMe)_3]$ finds its congeners in coordinated d/f metal hydride species such as WH_{12} as well as the 18-electron cluster WAu_{12}, which have been observed in matrix studies or in the gas phase but are not accessible in preparative quantities at ambient conditions.[14,15]

This Forum Article is intended to supplement our previous work in this field by a short review and, in particular, by a comparison of the structures and bonding situations of the homoleptic, all-zinc-coordinated systems $[M(ZnR)_n]$ with their heteroleptic Zn/Ga mixed-coordinated congeners $[M(ZnR)_a(GaR)_b]$ $(a + 2b = n \geq 8)$. Different from other highly coordinated complexes, the bonding ligand−ligand interactions in these compounds play an important role, not only reducing ligand−ligand repulsions but indeed adding an important contribution to the stability of the whole complexes. From this point of view, a more quantitative evaluation and comparison of the coordination polyhedra found for homoleptic $[M(ZnR)_n]$ and heteroleptic $[M(ZnR)_a(GaR)_b]$ as well as a discussion of their electronic structure in light of these coordination geometries is important.[9,12]

2. COORDINATION GEOMETRIES OF METAL-RICH COMPLEXES $[M(ZnR)_n]$ and $[M(ZnR)_a(GaR)_b]$

Figure 1 shows the molecular structures of homoleptic complexes $[M(ZnR)]_n$ of some second-row transition metals, i.e., $[Mo(ZnCp^*)_3(ZnMe)_9]$ (**$MoZn_{12}$**), $[Ru(ZnCp^*)_4(ZnMe)_6]$ (**$RuZn_{10}$**), $[Rh(ZnCp^*)_3(ZnMe)_6]$ (**$RhZn_9$**), and $[Pd(ZnCp^*)_4(ZnMe)_4]$ (**$PdZn_8$**). At first glance, each complex adopts a symmetry that is equivalent to the respective *closo*-borane structure, i.e., a regular icosahedron for **$MoZn_{12}$**, a bicapped square antiprism for **$RuZn_{10}$**, a tricapped trigonal prism for **$RhZn_9$**, and a dodecahedron for **$PdZn_8$**. The organic groups at the Zn atoms are, in almost all cases, arranged in such a way that the bulky Cp* groups occupy sites most distant from each other, which leads to overall symmetries of D_{3h} (**$MoZn_{12}$**, **$RhZn_9$**), C_s (**$RuZn_{10}$**), and D_{2h} (**$PdZn_8$**).

All of these complexes perfectly fullfill the 18 valence-electron (VE) rule. The simplest approach for electron counting is to consider the complexes as coordination compounds of one-electron-donor ZnR ligands to transition-metal centers in the oxidation state M^0. For each additional electron that is attributed by the central metal, the number of coordinating ZnR ligands is reduced by 1, resulting in an identical electron count of 18 for all complexes.

Besides these four cases of homoleptic complexes $[M(ZnR)_n]$, also three examples of "heteroleptic" Ga/Zn mixed compounds $[M(ZnR)_a(GaR)_b]$ $(a + 2b = n$ if compounds of the same metal M are compared) are known, i.e., $[Mo(GaMe)_4(ZnCp^*)_4]$ (**$MoGa_4Zn_4$**), $[Mo(GaMe)_2(ZnMe)_4(ZnCp^*)_4]$ (**$MoGa_2Zn_8$**), and $[Rh(GaMe)(ZnMe)_3(ZnCp^*)_4]$ (**$RhGaZn_7$**) (Figure 2). In all three cases, regular polyhedral coordination environments of central metals very similar to the parent $[M(ZnR)_n]$ are observed, i.e., trigonal dodecahedron for **MoGa4Zn$_4$** and **$RhGaZn_7$** (n = 8, M = Pd) and a centaur polyhedron (see later) for **$MoGa_2Zn_8$** (n = 10, M = Ru). Also, these complexes are regular 18 VE complexes and can be formally derived from respective homoleptic all-zinc complexes by the substitution of two one-electron-donor ZnR ligands by one two-electron-donor GaR ligand.

First, it shall be checked quantitatively to which degree **$PdZn_8$**, **$MoGa_4Zn_4$**, and **$RhGaZn_7$** as well as **$MoGa_2Zn_8$** and **$RuZn_{10}$**, respectively, are indeed isostructural and their coordination polyhedra are representations of ideal (mathematical) polyhedra. The term "ideal polyhedron" in all cases refers to a mathematical body with equal M−Zn distances; i.e., in some cases, two (or more) different Zn−Zn distances result as a consequence. This definition is quite reasonable when dealing with high-coordinate complexes. Alternatively, however, and especially in describing solid-state materials such as Hume−Rothery phases (vide infra), it might be more appropriate to define the "ideal polyhedron" based on equal Zn−Zn distances with varying M−Zn distances. However, it should be noted that this can result in polyhedra with unreasonably high differences of M−Zn distances, which obviously excludes such polyhedra to serve as models for coordination polyhedra of molecular compounds. The Cartesian coordinates of all ideal polyhedra used in our discussion below can be found in the Supporting Information. There are several approaches to identifying the degree of similarity of different polyhedra. For instance, it has been shown that the ratio of the volume of a polyhedron and that of a similar ideal mathematical body can serve as a quantitative measure for the discrepancy of these two bodies. However, the most widely used method is that of

dx.doi.org/10.1021/ic200800e |*Inorg. Chem.* 2011, 50, 12296–12302

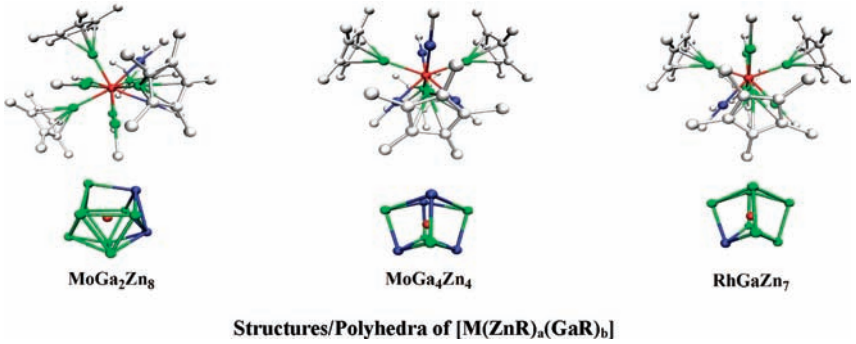

Figure 2. Perspective plot of the molecular structures $[Mo(GaMe)_4(ZnCp^*)_4]$, $[Mo(GaMe)_2(ZnMe)_4(ZnCp^*)_4]$, and $[Rh(GaMe)(ZnMe)_3(ZnCp^*)_4]$ in the solid state with the corresponding metal-core polyhedra ($MoGa_2Zn_8$), ($MoGa_4Zn_4$), and ($RhGaZn_7$) at the bottom. Color code: transition metals, red; Zn, green; Ga, blue; C, gray.

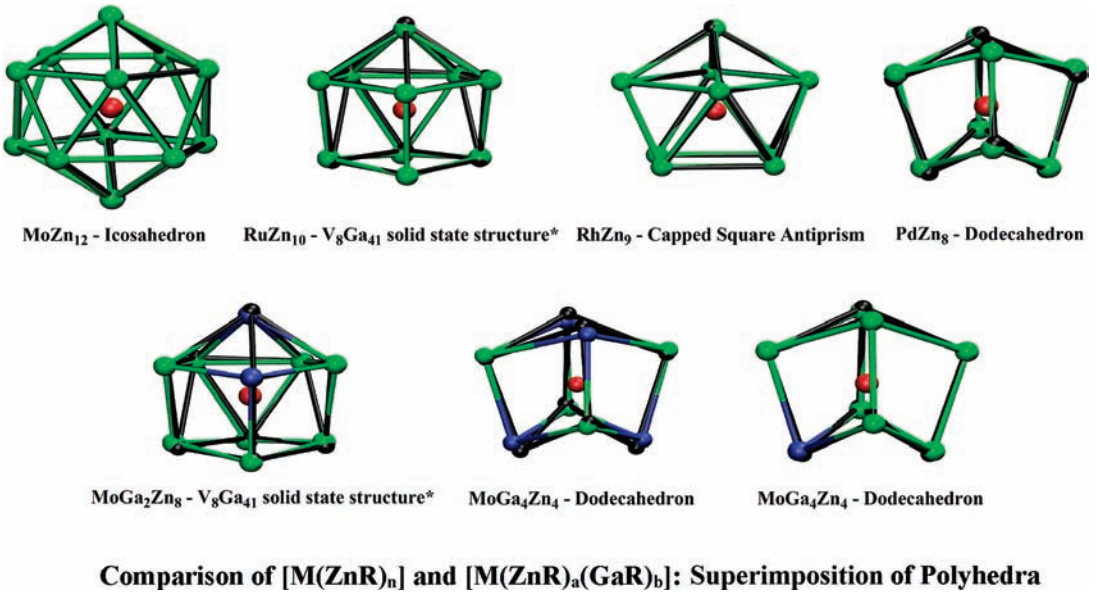

Figure 3. Orthographic plot of the superimpositions of the metal-core polyhedra (colored) and the corresponding ideal polyhedra (black). (*) For reference to the VGa_{10} polyhedra of the phase V_8Ga_{41}, see Table 1.

continuous-shape measures.[16−18] In this method, N vertices of a coordination polyhedron are given by their position vectors Q_i ($i = 1, 2, 3 ..., N$), as well as N vertices of an ideal polyhedron with the position vectors P_i ($i = 1, 2, 3 ..., N$).[5] The smallest distance $S_Q(P)$ of the position vectors between both polyhedra is expressed as

$$S_Q(P) = \frac{1}{N} min \sum_{i=1}^{N} |\vec{Q_i} - \vec{P_i}|^2 \times 100$$

All analyzed polyhedra were centered in the origin and standardized ($|\vec{V_i}| = |\vec{V_j}|/|\vec{V_j}|$) prior to all calculations; therefore, the usual scaling factor has been omitted. Final values of $0 \leq S_Q(P) \leq 100$ can be obtained and serve as a quantitative measure for the shape of the experimental polyhedron derived from single-crystal X-ray diffraction studies. With $S_Q(P) = 0$, the polyhedron represents the exact ideal shape, while increasing values denote increasing distortions. In our approach, we have chosen a computer-aided method for finding the minimum distance, i.e., for identifying the best superimposition of the experimental and ideal polyhedron: The two polyhedra with the transition-metal center in the origin were superimposed. One of the two polyhedra is then rotated around three independent axes by 360° in steps of $360/n$ degrees, resulting in n^3 different superimpositions. For each step, a "minimum distance" of the polyhedral vertices is calculated by permutation of all plausible vertex combinations. This procedure results in n^3 distance values, with the smallest one representing the most ideal superimposition of the two polyhedra. For this superimposition, the shape measure $S_Q(P)$ is calculated as described above. Figure 3 shows the most ideal superpositions for each compound, with $S_Q(P)$ being the global minimum. Table 1 gives a summary of the shape measures $S_Q(P)$ for all complexes $[M(ZnR)_n]$ and $[M(ZnR)_a(GaR)_b]$ with a comparison of the experimental and calculated structures (see the DFT section below).

According to Alvarez et al., who performed extensive studies on the structures of various highly coordinated metal complexes, shape measures $S_Q(P)$ below 1.0 indicate minor distortions from

dx.doi.org/10.1021/ic200800e |Inorg. Chem. 2011, 50, 12296–12302

Table 1. Shape Measures $S_Q(P)$ for the Comparison of Ideal Polyhedra with Experimental and Calculated Structures Based on the DFT with R = H: MZn_8, Mo_4Ga_4, $RhGaZn_7$, $RuZn_{10}$, $MoGa_2Zn_8$, $MoZn_{12}$(Me), and $MoZn_{12}$(Et)

		$S_Q(P)$	
compound	ideal shape	exptl	calcd
$NiZn_8$	dodecahedron	0.53	
$PdZn_8$	dodecahedron	0.20	2.66
$PdZn_8$	square antiprism	2.85	0.19
$PtZn_8$	dodecahedron	0.15	
$MoGa_4Zn_4$	dodecahedron	0.91	0.16
$RhGaZn_7$	dodecahedron	0.15	2.26
$RhZn_9$	tricapped trigonal prism	0.96	0.00
$RhZn_9$	capped square antiprism	0.04	0.96
$RuZn_{10}$	bicapped square antiprism	3.55	0.70
$RuZn_{10}$	4A,6B-extended dodecahedron	1.59	3.02
$RuZn_{10}$	V_8Ga_{41} solid-state structure[a]	0.33	3.16
$MoGa_2Zn_8$	ibicapped square antiprsm	3.94	4.11
$MoGa_2Zn_8$	4A,6B-extended dodecahedron	2.05	2.42
$MoGa_2Zn_8$	V_8Ga_{41} solid-state structure[a]	0.33	0.58
$MoZn_{12}$(Me)	icosahedron	0.05	0.00
$MoZn_{12}$(Et)	icosahedron	0.09	

[a] A VGa_{10} coordination polyhedron extracted from the sold-state structure of V_8Ga_{41} has been used as a model for a centaur polyhedron (half-cube half-icosahedron) and compared to the molecular structures of the 10-fold-coordinated molecular structures.[19]

the ideal shape, while $1.0 < S_Q(P) < 3.0$ indicates important distortions, however, with the ideal shape still providing a suitable stereochemical description.[20] Thus, homoleptic 8-fold-coordinated $[M(ZnR)_8]$ and heteroleptic 8-fold-coordinated **$MoGa_4Zn_4$** and **$RhGaZn_7$** all represent regular dodecahedra with only minor distortions, independent of the d-electron count of the central metal. The polyhedron of **$RhZn_9$** is an almost perfect capped square antiprism, while also the tricapped trigonal prism represents a suitable description, yet with higher distortions. Complexes **$MoZn_{12}$** are almost perfectly icosahedral, with the difference of the shape measures for $[Mo(ZnMe)_9(ZnCp^*)_3]$ [**$MoZn_{12}$(Me)**, $S_Q(P) = 0.05$] and the sterically less crowded $[Mo(ZnEt)_{10}(ZnCp^*)_2]$ [**$MoZn_{12}$(Et)**, $S_Q(P) = 0.09$] being negligible. In sharp contrast, all 10-fold-coordinated complexes show major distortions from ideal shapes.[21] **$RuZn_{10}$** and **$MoGa_2Zn_8$** can both be described as a 4A,6B-extended dodecahedron [$S_Q(P) = 1.59$ and 2.05, respectively], although the high values for $S_Q(P)$ indicate strong distortions. It should be noted that the geometries of 10-fold-coordinated complexes are generally considered to be more or less problematic and can often not be described in terms of one ideal shape. As suggested by one reviewer of this manuscript, the 10-fold-coordinated metal centers in solid-state structures are often described by so-called centaur polyhedra, which are constructed by fusing two (more or less) ideal polyhedra together, e.g., one cube and one icosahedron, to give a 10-vertex body. The comparison of the coordination polyhedra of **$RuZn_{10}$** and **$MoGa_2Zn_8$** with a **VGa_{10}** polyhedron extracted from the solid-state structure of V_8Ga_{41}[19] indeed shows a very good agreement. Most interestingly, some polyhedra of the calculated structures (vide infra) are not consistent with the polyhedra of the experimentally determined structures. While for **$MoZn_{12}$** both calculated and experimental structures are almost perfectly icosahedral, the difference is most prominent for the **MZn_8** polyhedra, which are almost perfectly dodecahedral in the experimental structures while calculations predict a perfect square-antiprismatic structure. This is most likely due to the fact that the hydrides $[M(ZnH)_n]$ have been used as models for the calculated structures, which experience less steric strain than the experimentally observed molecules $[M(ZnMe)_a(ZnCp^*)_b]$ $(a + b = n)$. However, the calculated structures $[Pd(ZnMe)_8]$ with eight identical ligands with larger steric demand than ZnH also exhibit square-antiprismatic minimum structures.

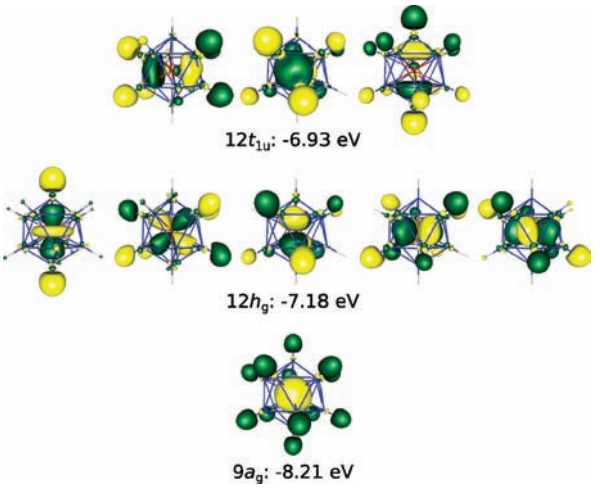

Figure 4. Three highest sets of MOs of the parent compound $[Mo(ZnH)_{12}]$.

3. ELECTRONIC STRUCTURES OF $[M(ZnR)_a(GaR)_b]$

A useful starting point for understanding the bonding situation in the homoleptic complexes $[M(ZnH)_n]$ and in the heteroleptic congeners $[M(ZnH)_a(GaH)_b]$ $(a + 2b = n)$ is the icosahedral species $[Mo(ZnH)_{12}]$, which presents a reasonable model compound for icosahedrally coordinated complexes $[Mo(ZnR)_{12}]$.[8−10] Figure 4 shows three sets of highest occupied molecular orbitals (HOMOs) of $[Mo(ZnH)_{12}]$, which exhibit all relevant features of the chemical bonding. Because of the icosahedral symmetry of $[Mo(ZnH)_{12}]$, s-, p-, and d-type orbital interactions of molybdenum are easily assigned because they belong to different irreducible representations of the I_h point group. The HOMO ($12t_{1u}$) represents Zn−H and Zn−Zn interactions, with only very minor contributions of the p atomic orbitals (AOs) of Mo. The quintuply degenerated ($12h_g$) HOMO−1 has large contributions of the d AOs of Mo that mix with the sp^x-hybridized AOs of Zn. The HOMO−2 ($9a_g$) signifies interactions of the Zn cage with Mo via its valence s AO.

An energy decomposition analysis (EDA) of interactions between the Mo atom and the $(ZnH)_{12}$ cage quantitatively supports the spatial analysis of the orbitals. The EDA results suggest that the HOMO (t_{1u}) orbital contributes little to the Mo ← $(ZnH)_{12}$ bonding, which means that the charge donation of $(ZnH)_{12}$ into the p AOs of Mo is very small. The HOMO represents Zn−H besides Zn−Zn bonding interactions that are important for the stability of the cage, which explains the unusually high coordination number. The HOMO is not important for the Mo−$(ZnH)_{12}$ bonding though.[9] The most important orbital stabilization for

dx.doi.org/10.1021/ic200800e |*Inorg. Chem.* 2011, 50, 12296–12302

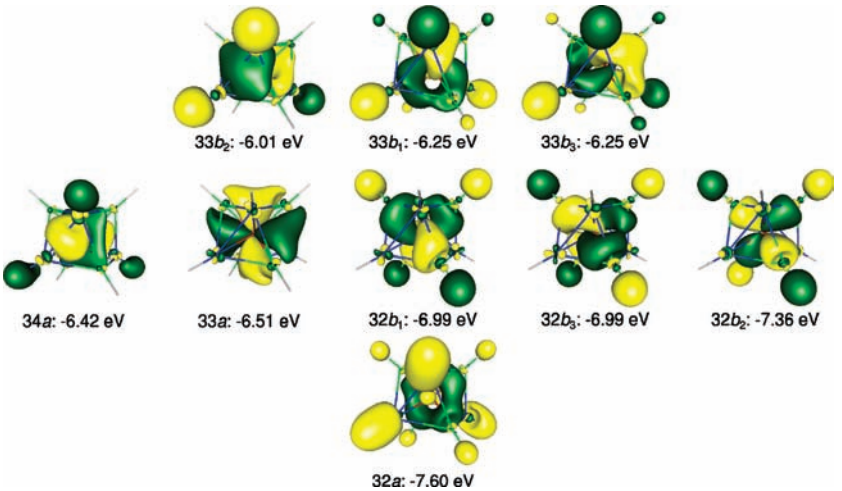

Figure 5. Selected valence MOs of $[Mo(GaH)_4(ZnH)_4]$. Color code: green, Ga; blue, Zn; red, Mo. Isosurfaces at 0.033 au.

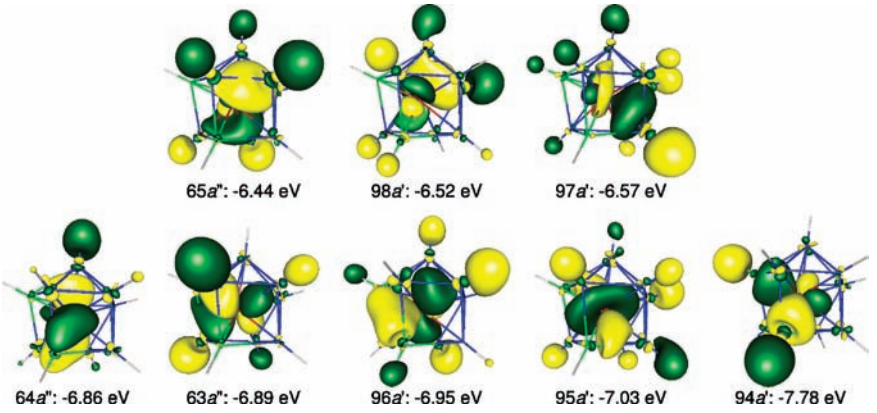

Figure 6. Selected valence MOs of $[Mo(GaH)_2(ZnH)_8]$. Color code: green, Ga; blue, Zn; red, Mo. Isosurfaces at 0.033 au.

Mo−$(ZnH)_{12}$ bonding comes from the HOMO−1 (h_g) and HOMO−2 (a_g). It follows that the metal−ligand interactions come mainly from the s and d AOs of Mo, while the p AOs are less important. The same conclusion about metal−ligand interactions has been made in a detailed bonding analysis of the isoelectronic hexacarbonyls $[M(CO)_6]^q$ for the metals M^q = Hf^{2-}, Ta^-, W, Re^+, Os^{2+}, Ir^{3+}.[22]

The six electrons in the triply degenerated $12t_{1u}$ HOMO of $[Mo(ZnH)_{12}]$ are distributed over 30 direct Zn−Zn interactions in $[Mo(ZnH)_{12}]$, which leaves only 0.1 electron pair for each Zn−Zn "bond". This explains why the AIM analysis[23] of the latter compound does not show tangential Zn−Zn bond paths.[9] The same bonding model as $[Mo(ZnH)_{12}]$ is also valid for the lower coordinated homologues $[M(ZnH)_n]$ (M = Ru, Rh, Ni, Pd, Pt; n = 10, 9, 8). All compounds $[M(ZnH)_n]$ show an absence of tangential Zn−Zn bond paths according to AIM. The lower symmetry of the latter systems yields MOs, which belong to an irreducible representation of the point groups where the s, p, and d AOs of the central atoms are not strictly separated. Thus, there is no clear-cut separation between the M(AO)−Zn interactions for different AOs. However, analysis of the electronic structures of all $[M(ZnH)_n]$ compounds shows that the p AOs of the central atom M play a negligible role for the M−Zn interactions that come mainly from the s and d AOs.[8,10]

The same conclusion as that for $[M(ZnH)_n]$ can be made for the mixed complexes $[M(ZnR)_a(GaR)_b]$, which have a still lower symmetry than the homoleptic compounds. As examples, we show the highest-lying occupied valence Kohn−Sham MOs of $[Mo(GaH)_4(ZnH)_4]$ (D_2 symmetry; Figure 5), $[Mo(GaH)_2(ZnH)_8]$ (C_s symmetry; Figure 6), and $[Rh(GaH)(ZnH)^7]$ (C_s symmetry; Figure 7).

In the D_2 point group, the s, d_{z^2}, and $d_{x^2-y^2}$ AOs of the central atom M are in the same irreducible representation a, while one p AO and one d AO mix in each b_n irreducible representation (n = 1−3). Thus, the assignment of MOs corresponding to s-, p-, and d-type interactions can only be made in an approximate fashion. However, visual inspection of the graphical display of the MOs and numerical analysis of the AO coefficients of the orbitals show that the bonding situation in the molecules is similar to that in the homoleptic complexes. In the D_2-symmetric compound $[Mo(GaH)_4(ZnH)_4]$, the HOMOs can be arranged as three sets of orbitals, as shown in Figure 5, that are analogous to the orbitals for $[Mo(ZnH)_{12}]$, which are displayed in Figure 4. The three HOMOs $33b_2$, $33b_1$, and $33b_3$, which exhibit a shape similar to that of the $12t_{1u}$ HOMO of $[Mo(ZnH)_{12}]$, represent mainly M′−H, M′−M′, and M′−Mo_p interactions (M′ = Zn, Ga). The coefficients of the p AOs of Mo in $33b_2$, $33b_1$, and $33b_3$ are very small, which indicates that these orbitals play a minor role for

dx.doi.org/10.1021/ic200800e |*Inorg. Chem.* 2011, 50, 12296–12302

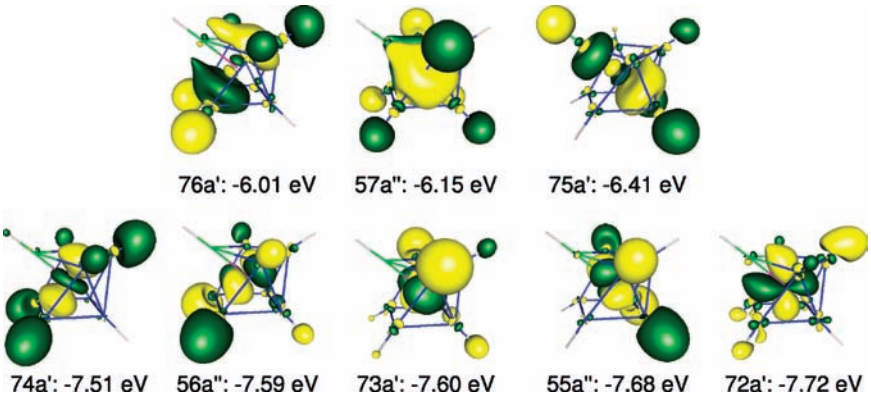

Figure 7. Selected valence MOs of $[Rh(GaH)(ZnH)_7]$. Color code: green, Ga; blue, Zn; red, Mo. Isosurfaces at 0.033 au.

$Mo-(ZnH)_{12}$ interactions. The five orbitals $34a'-32b_2$ (Figure 5) signify bonding between the d AOs of Mo and ZnH as well as GaH moieties. The orbital 32a, which stands also for $Mo-(GaH)_4(ZnH)_4$ bonding, has a large coefficient from the valence s AO of Mo.

The mixed complex $[Mo(GaH)_2(ZnH)_8]$ has only C_s symmetry, which makes the assignment of the orbitals to specific interactions more difficult than for $[Mo(GaH)_4(ZnH)_4]$. Yet, the shape of the MOs and inspection of the AOs in the valence orbitals show that the bonding situation in the former complex is similar to that in the latter. Figure 6 shows two sets of energetic HOMOs of $[Mo(GaH)_2(ZnH)_8]$. They have been arranged in the same way as the two highest-lying 3/5 sets of $[Mo(GaH)_4(ZnH)_4]$ (Figure 5) because they can be easily identified as related pairs. The Mo AO coefficients in the triple $65a''/97a'/98a'$ are quite small; the orbitals represent mainly $M'-H$ and $M'-M'$ interactions (M' = Zn, Ga). The next five orbitals signify mainly interactions of Zn/Ga with the Mo d orbitals. We could not identify a MO that has a large coefficient of the valence s AO of Mo. This is probably because of the C_s symmetry of $[Mo(GaH)^{2-}(ZnH)_8]$, where large s/p/d mixing is observed in all orbitals. The AIM analysis of the latter compound does not show any $M'-M'$ bond paths.

A similar situation as that in $[Mo(GaH)_2(ZnH)_8]$ is also found for the rhodium complex $[Rh(GaH)(ZnH)_7]$, which has also C_s symmetry. The MOs of the latter complex actually look quite similar to those of $[Pd(ZnH)_8]$, which have been discussed before.[8] Figure 7 shows two sets of the energetic HOMOs of $[Rh(GaH)(ZnH)_7]$, which can be easily identified as related pairs of the two highest-lying 3/5 sets of $[Mo(GaH)_2(ZnH)_8]$ (Figure 6).

The three HOMOs 75a′, 76a′, and 57a″ signify $M'-H$ and $M'-M'$ interactions (M' = Zn, Ga); the AO contributions of Rh are negligible. The shape of the quintuple 74a′, 56a″, 73a′, 55a″, and 72a′ reveals the large contributions of the Rh d AOs, which mix with the $M'H$ orbitals. There is no MO, however, that has a prominently large coefficient of the valence s AO of Rh, which is rather distributed in numerous orbitals. AIM analysis gives only bond paths for $Rh-M'$ and $M'-H$ interactions but not for $M'-M'$.

4. CONCLUSION

The icosahedral complex $[Mo(ZnMe)_9(ZnCp^*)_3]$ has been discussed as the prototype for a whole family of high-coordinate, metal-rich compounds $[M(ZnR)_n]$ ($n \geq 8$). Different from other highly coordinate complexes of classic monodentate (nonchelating) nonmetal ligator ligands, the (weakly) bonding ligand−ligand interactions between the Zn atoms in these compounds play an important role. DFT calculations reveal that the three HOMOs are very similar for all complexes $[M(ZnR)_n]$, independent of the coordination number and particular structure. The six electrons in those three HOMOs are distributed over all direct Zn−Zn interactions, leaving only $3/n$ electron pairs for each Zn−Zn interaction in a polyhedron with n edges. The next five HOMOs represent the constructive interaction of the metal d orbitals with the zinc shell. The two sets of orbitals might be triply and quintuply degenerate, as in the case of icosahedral $[Mo(ZnH)_{12}]$, or nondegenerate, as found in complexes with lower symmetry. As a consequence of this electronic situation, the structures and coordination polyhedra of $[M(M'R)_n]$ (M' = Zn, Ga) are *independent* of the central metal or the nature of the metals M' in the ligand shell. For instance, the 18 VEs of $[Mo(GaR)_4(ZnR)_4]$, $[Rh(ZnR)_7(GaR)]$, and $[M(ZnR)_8]$ (M = Ni, Pd, Pt) may be formally attributed differently from the central metal and the ligand shell, respectively (Mo d^6/12 VE for Ga_4Zn_4; Rh d^9/9 VE for $GaZn_7$; Pd d^{10}/8 VE for Zn_8), yet the resulting MO schemes differ only slightly as a result of different symmetry restrictions, resulting in the same coordination polyhedra (structures) for all complexes. Such an electronic structure may be viewed as a molecular representation for the situation in extended solid-state intermetallic phases of the Hume−Rothery type, where quite similar structural features are observed in the case of different metal combinations, which, however, provide similar VE concentrations. For example, the electronic structure of the alloy phase V_8Ga_{41} has been described as the interaction of V d orbitals with the delocalized electrons of a Ga-atom matrix.[19,23] Furthermore, the Ga atoms in this alloy can be partially substituted for Zn atoms without structural changes; thus, $Mn_8Ga_{41-x}Zn_x$ is isostructural to V_8Ga_{41}. This is (at least conceptually) quite similar to the connection between the composition, electronic bonding situation, and structure for the complexes $[M(ZnR)_n]$ and $[M(ZnR)_a(GaR)_b]$, as discussed above. From this point of view, the preparation of more extended mixed-metal clusters $[M_a(ZnR)_b]$ and $[M_a\{(ZnR)_p(GaR)_q\}]$ ($a > 1$; $p + 2q = b < n$) incorporating more than one transition-metal atom M embedded in a matrix of Zn (Cd, Hg) and Ga (Al, In) "alloy" atoms (and other metal-atom ligator ligands $M'R'$ being isolobal to ZnR or GaR, such as MgR and $AuPR'_3$) is a valuable target, which remains a challenge to the synthetic, organometallic, and materials chemist.

dx.doi.org/10.1021/ic200800e |*Inorg. Chem.* 2011, 50, 12296–12302

It will be interesting to see how the electronic structures of such more extended "metal-atom-rich molecules" develop features gradually more and more related to some corresponding intermetallic solid-state phases.

■ ASSOCIATED CONTENT

Supporting Information. Computational details, Cartesian coordinates, and additional references. This material is available free of charge via the Internet at http://pubs.acs.org.

■ AUTHOR INFORMATION

Corresponding Author

*E-mail: frenking@chemie.uni-marburg.de (G.F.), roland.fischer@ruhr-uni-bochum.de (R.A.F.). Fax (+49)234 321 4174.

■ ACKNOWLEDGMENT

This work was funded by the German Research Foundation (joint project of R.A.F. and G.F. on "Metal Rich Molecules"). The dissertation project of M.M. is supported by German Chemical Industry Fund (fellowship) and the Ruhr University Research School (http://www.research-school.rub.de).

■ REFERENCES

(1) Elschenbroich, C. *Organometallics*; Wiley-VCH: New York, 2006.
(2) Cotton, F. A.; Wilkinson, G. *Advanced Inorganic Chemistry*, 6th ed.; Wiley India Pvt. Ltd.: New Delhi, India, 2007.
(3) Gispert, J. R. *Coordination Chemistry*; Wiley-VCH: New York, 2008.
(4) Huheey, J. E.; Keiter, E. A.; Steudel, R.; Keiter, R. *Anorganische Chemie: Prinzipien von Struktur und Reaktivität*; De Gruyter: Berlin, 2003.
(5) Drew, M. G. B. *Coord. Chem. Rev.* **1977**, *24*, 179–275.
(6) Muetterties, E. L.; Wright, C. M. *Q. Rev., Chem. Soc.* **1967**, *21*, 109–194.
(7) Lippard, S. J. *Prog. Inorg. Chem.* **1967**, *8*, 109–193.
(8) Cadenbach, T.; Bollermann, T.; Gemel, C.; Tombul, M.; Fernandez, I.; von Hopffgarten, M.; Frenking, G.; Fischer, R. A. *J. Am. Chem. Soc.* **2009**, *131*, 16063–16077.
(9) Cadenbach, T.; Bollermann, T.; Gemel, C.; Fernandez, I.; von Hopffgarten, M.; Frenking, G.; Fischer, R. A. *Angew. Chem., Int. Ed.* **2008**, *47*, 9150–9154.
(10) Gonzalez-Gallardo, S.; Prabusankar, G.; Cadenbach, T.; Gemel, C.; von Hopffgarten, M.; Frenking, G.; Fischer, R. In *Metal−Metal Bonding*; Parkin, G., Ed.; Springer: Berlin/Heidelberg, 2010; Vol. 136, pp 147−188.
(11) Bollermann, T.; Cadenbach, T.; Gemel, C.; von Hopffgarten, M.; Frenking, G.; Fischer, R. A. *Chem.—Eur. J.* **2010**, *16*, 13372–13384.
(12) Cadenbach, T.; Gemel, C.; Fischer, R. A. *Angew. Chem., Int. Ed.* **2008**, *47*, 9146–9149.
(13) Molon, M.; Cadenbach, T.; Bollermann, T.; Gemel, C.; Fischer, R. A. *Chem. Commun.* **2010**, *46*, 5677–5679.
(14) Gagliardi, L.; Pyykkö, P. *J. Am. Chem. Soc.* **2004**, *126*, 15014–15015.
(15) Pyykkö, P.; Runeberg, N. *Angew. Chem., Int. Ed.* **2002**, *41*, 2174–2176.
(16) Zabrodsky, H.; Peleg, S.; Avnir, D. *J. Am. Chem. Soc.* **1992**, *114*, 7843–7851.
(17) Zabrodsky, H.; Peleg, S.; Avnir, D. *J. Am. Chem. Soc.* **1993**, *115*, 8278–8289.
(18) Pinsky, M.; Avnir, D. *Inorg. Chem.* **1998**, *37*, 5575–5582.
(19) Häussermann, U.; Viklund, P.; Svensson, C.; Eriksson, S.; Berastegui, P.; Lidin, S. *Angew. Chem.* **1999**, *111*, 580–584.
(20) Cirera, J.; Ruiz, E.; Alvarez, S. *Organometallics* **2005**, *24*, 1556–1562.
(21) Ruiz-Martínez, A.; Alvarez, S. *Chem.—Eur. J.* **2009**, *15*, 7470–7480.
(22) Diefenbach, A.; Bickelhaupt, F. M.; Frenking, G. *J. Am. Chem. Soc.* **2000**, *122*, 6449–6458.
(23) Bader, R. F. W. *Atoms in Molecules. A Quantum Theory*; Oxford University Press: Oxford, U.K., 1990.
(24) Ferro, R.; Saccone, A.; Cahn, R. W.; Haasen, P.; Kramer, E. J. *Materials Science and Technology*; VCH: Weinheim, Germany, 1993.